

Towards Coordinated Vision-based Docking Using an Autonomous Surface Vehicle

Matthew Dunbabin[†], Brenton Lang[‡] and Brett Wood[‡]

[†]Autonomous Systems Laboratory, CSIRO ICT Centre, P.O. Box 883, Kenmore, QLD 4069, Australia.

[‡]School of Engineering, Griffith University, Australia.

matthew.dunbabin@csiro.au, brenton.lang@student.griffith.edu.au, brett.wood2@student.griffith.edu.au

Abstract

This paper describes the development and experimental evaluation of a novel vision-based Autonomous Surface Vehicle with the purpose of performing coordinated docking manoeuvres with a target, such as an Autonomous Underwater Vehicle, on the water's surface. The system architecture integrates two small processor units; the first performs vehicle control and implements a virtual force obstacle avoidance and docking strategy, with the second performing vision-based target segmentation and tracking. Furthermore, the architecture utilises wireless sensor network technology allowing the vehicle to be observed by, and even integrated within an ad-hoc sensor network. The system performance is demonstrated through real-world experiments.

1 Introduction

This paper describes the first step in the realisation of an Autonomous Surface Vehicle (ASV) to carry multiple Autonomous Underwater Vehicles (AUVs) through the development and experimental validation of a coordinated vision-based docking and control strategy to allow automated retrieval of a surfaced AUV.

For many years, AUVs have been researched and deployed extensively in our oceans. However, it is long been recognized to maintain accurate localization whilst underwater requires significant logistical support from the surface. Traditionally, this has been provided using chase ships or deploying underwater acoustic beacons to maintain communication with, and position the AUVs.

In more recent times, there has been increasing interest in using Autonomous Surface Vehicles (ASVs) to provide an automated solution to the task of integrated communication between surface and subsurface robotic vehicles. Examples include the MIT SCOUT ASV [Curcio *et al.*, 2005a; 2005b] where a series of automated kayaks demonstrated moving baseline navigation for use by the Odyssey AUV. A

similar study was conducted by Pascoal *et al.* [Pascoal *et al.*, 2000] using a catamaran style vessel, with other applications such as [Bishop, 2004] considering the formation control of ASVs for marine security applications.

A review of ASV technology by Caccia [Caccia, 2006], describes how ASV prototype systems have been developed for both research and military applications. Typically, the research class of ASVs are lower speed catamaran style vehicles, with the military vehicles generally being faster, monohull designs. The primary areas of research identified in the literature have focused on vehicle design and construction [Curcio *et al.*, 2005a; Larson *et al.*, 2006; Manley *et al.*, 2000; Leonessa *et al.*, 2003; Reed *et al.*, 2006], navigation and control [Vaneck, 1997; Alves *et al.*, 2006; Reyhanoglu and Bommer, 2006] and path-planning and obstacle avoidance [Larson *et al.*, 2006].

However, we have identified an opportunity to develop novel systems that extend the capabilities of an ASV to deploy, recover and transport AUVs. This would significantly improve the operational logistics associated with offshore underwater and surface robotic systems and is the focus of this paper.

Figure 1 shows an illustration of the CSIRO multi-AUV carrying ASV concept. The purpose of this robotic system is to carry a number, typically 4, Starbug AUVs [Dunbabin *et al.*, 2005] to strategic locations for underwater monitoring tasks. Once at the location, the ASV automatically deploys an AUV, then moves to the next location to repeat the process. At the completion of the mission, the AUV surfaces and rendezvous with the ASV. At this point, the two vehicles coordinate their actions to dock together and the AUV is lifted out of the water. The AUV's data is then downloaded and it is recharged from the ASV's onboard solar panels whilst being transported to the next survey location.

There are a number of research challenges relating to both the AUV and ASV to realize this coordinated control. Considered here is the first step in enabling an ASV to automatically detect a target, such as an AUV, floating on the surface and robustly manoeuvre itself over the target for collection. As an initial approach to target identification a vision-based

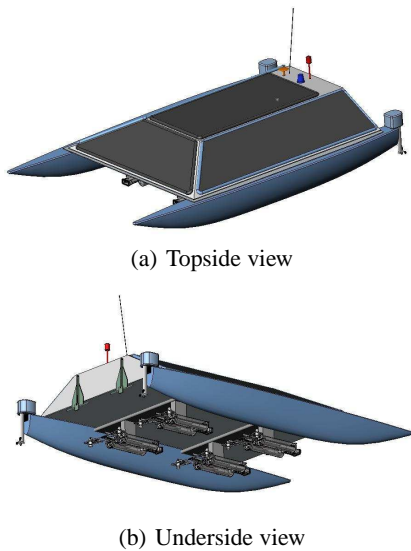


Figure 1: The CSIRO multi-AUV carrying ASV concept. The top surface of is covered in solar panels for recharging the AUVs, which are carried on the underside of the ASV.

solution was adopted.

A recent study by Martins et al [Martins *et al.*, 2007] also considers a vision system for the docking control of an ASV and they provide some experimental results of the system in docking with a torpedo style AUV. Our solution differs from [Martins *et al.*, 2007] in that we desire the entire system to operate from a series of distributed low-power processors, and therefore, the vision and vehicle control systems proposed use different approaches for image segmentation and trajectory control.

1.1 Paper Outline

The remainder of this paper is structured as follows; Section 2 describes the general construction of the Starship ASV. Section 3 overviews the vision-based target identification system, with Section 4 describing the Virtual Force Field vehicle control strategy. Experimental performance of the systems in pool and lake environments given in Section 5, and finally, Section 6 concludes the paper.

2 Starship ASV

In order to prove the vision and control systems, a small low-cost ASV was developed. The prototype design, known as Starship, is of a twin hull (catamaran style) construction that can allow the target, an AUV in this scenario, to fit between two hulls for deployment, retrieval and transportation. Figure 2 shows the actual Starship ASV prototype used in this study.

The ASV is 2.0m long and 1.3m wide with the hulls constructed from PVC pipe. The vehicle's buoyancy is such that it has additional capacity to lift a 30kg target out of the wa-



Figure 2: The Starship ASV prototype.

ter. Propulsion is provided by two fixed commercial AUV thrusters, manufactured by Seabotix, located at the rear of the vehicle, one on each hull. These provide forward as well as rotational actuation through differential control of the motors. The camera system is installed on top of a tripod and slanted downward to allow improved field-of-view for target detection in the water. The vehicle's power is provided by a series of batteries stored in the tubes on the top of each hull.

The system architecture, as illustrated in Figure 3, consists of three primary components; the ASV controller, the vision system, and the base station.

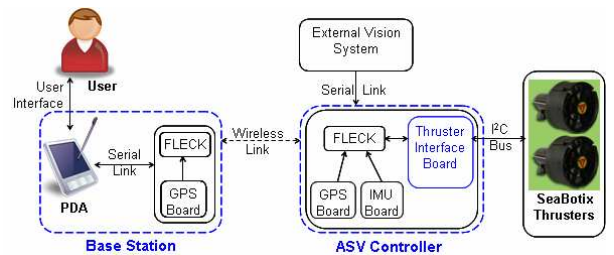


Figure 3: ASV prototype system architecture.

The ASV controller uses the FleckTM [Corke *et al.*, 2007] wireless sensor network board as the core processor. This controller performs the vehicle control, obstacle avoidance, mission execution, and interfaces with external wireless sensor networks and the base station. The low-power FleckTM has many expansion boards such as a GPS and an inertial measurement unit (IMU) which are both used in this study. Furthermore, it has the ability to control the Seabotix thrusters through an I²C bus. These thrusters have an on-board processor which maintains a tight velocity control loop to a commanded setpoint. This allowed us to experimentally map the control input to actual thrust output.

The external vision system comprises of a OmniVision OV7640 color CMOS camera and a Blackfin 600MHz DSP processor. The Blackfin collects and processes the image

using the method described in Section 3. The vision system communicates the processed target tracking results to the FleckTM ASV controller via an RS232 serial link. The processor also has the ability to connect to an external Ethernet for debugging and viewing of raw and segmented images. Both the vision system and the ASV controller hardware components were packaged into water resistant housings as shown in Figure 4.

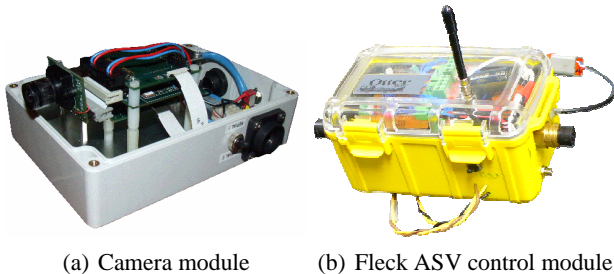


Figure 4: Blackfin DSP & CMOS camera vision system (without lid), and Fleck ASV controller modules.

A PDA connected serially to a Fleck is used as a base station for remote operation and observation of the ASV. The base station allowed rapid development and task assignment for the ASV with the ability to wirelessly set control gains and various docking parameters, as well as to observe the status of the vision system. Through the addition of a GPS, the base station also has the ability to act as a surrogate docking target for testing purposes.

3 Vision System

The target identification and tracking system was implemented on the Blackfin processor running a Linux operating system. The image capture and processing software was written using the DDX middleware [Corke *et al.*, 2004]. The ASV vision system has three primary functions: (1) Target segmentation from the image, (2) correction for camera lens distortion, (3) transformation from image coordinates to global coordinates.

3.1 Target Segmentation

As the desired target is primarily yellow in color, a color-based image segmentation technique was employed. The captured 640x480 pixel RGB Bayer image from the vision system was subsampled to 320x240 pixels and converted to the HSV color space for segmentation. HSV [Smith, 1978] was chosen for image segmentation due to better color constancy compared to other representations such as YUV. As yellow appears within an angular range in HS space, each pixel was evaluated and accepted if it was within a pre-specified color range. A closing operation was performed on the segmented image with the largest valid blob selected as the target. Figure 5(a) shows an example image showing the AUV target with Figure 5(b) showing the final segmented image.



(a) Original image (b) Final segmented image

Figure 5: Example of target segmentation using the ASV vision system.

3.2 Distortion correction

Due to significant barrel distortion experienced in the ASV vision system, the radial/tangential method as described by Cucchiara *et al.* [Cucchiara *et al.*, 2003] was used to correct the image. Instead of undistorting the entire image, only the segmented pixels from the previous section were corrected with the target area recalculated and the centroid of the target estimated.

3.3 Coordinate Transform

In order to estimate the position of the target with respect to the ASV, it was assumed that the target lay on a smooth flat plane at the water's surface. Furthermore, to simplify the analysis it was assumed that roll and pitch of the ASV are considered negligible, although an appropriate coordinate transform could compensate this by using the inertial measurement unit on the ASV controller module.

Figure 6 shows the basic geometry for the vision system on the ASV where the camera is located at a height h_c above the surface plane and is tilted at an angle θ_c down from the horizontal. The origin of the vehicle (camera) centred coordinate system is directly below the camera on the water's surface with the x -axis forward, and the y -axis out of the page.

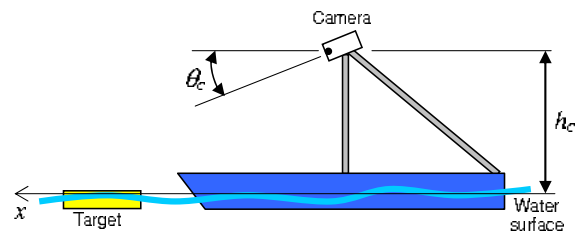


Figure 6: Geometry of the vision system on the ASV.

The coordinates of the target centroid with respect to the vehicle coordinate system (x_t, y_t) are given by

$$x_t = \frac{h_c}{\tan\left(\theta_c - \tan^{-1}\left(\frac{v_t}{f_v}\right)\right)} \quad (1)$$

$$y_t = \frac{-u_t d_{tx}}{f_u} \quad (2)$$

$$d_{tx} = \sqrt{h_c^2 + x_t^2} \quad (3)$$

where u_t and v_t are the centroid coordinates of the segmented image as determined in Section 3.2 (with the origin set at the center of the image), and f_u and f_v are the camera focal lengths in the camera u - and v -coordinates respectively.

4 ASV Docking Control

In order to dock with a target of interest, the vehicle must be capable of moving from its current pose, given by $\mathbf{P} = (x_{ss}, y_{ss}, \psi_{ss})$, to a desired global position and orientation angle, $\mathbf{P}^* = (x^*, y^*, \psi^*)$. Here the Cartesian position of the vehicle can be measured using either GPS or by resolving the relative vision-based position into the global coordinate system. The heading is measured from the Fleck IMU.

The ASV has two fixed parallel thrusters which are controlled independently. The motor forces have, through experiment, been determined to be linearly proportional to their on-board motor controller input.

The control inputs determined by the ASV controller are vehicle centric forces (F_v, F_ψ) which are the desired forward force and rotational force respectively. These vehicle centric forces are then translated to individual left and right motor forces (F_L, F_R). Figure 7 shows a top view illustration of the vehicle with the left and right control forces.

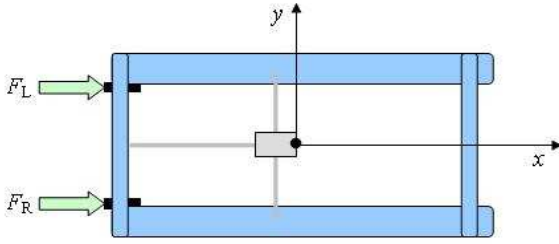


Figure 7: ASV thruster control forces (top view).

4.1 ASV Docking Motion Control

Due to the limited processing power of the ASV Controller, it was desired to use Virtual Force (or Potential) Fields (VFF) rather than a dedicated path planner to implement vehicle motion control. Virtual force fields have been used extensively for robot motion control [Borenstein and Koren, 1989]. The advantage of VFF's in this application are they are computationally simple to implement, and they allow the introduction of additional virtual forces to protect against collision with the target or avoid obstacles.

There are two virtual forces considered in this study, a linear attraction force (F_a) and an inverse square repelling force (F_r) given by

$$F_a = K_a \cdot r \quad (4)$$

$$F_r = \frac{K_r}{r^2} \quad (5)$$

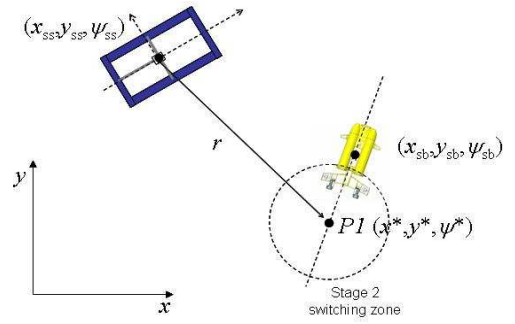
where r is the Euclidean distance between the ASV center-of-gravity to the action point of the virtual force, and K_r and K_a are constants representing the strength of the respective virtual forces.

The docking procedure is divided into two stages; The first stage is used to move the vehicle to within a pre-specified radius of the target, with the second stage providing the mechanism for the ASV to align with the target (ψ^*) and move over the target to complete the docking procedure.

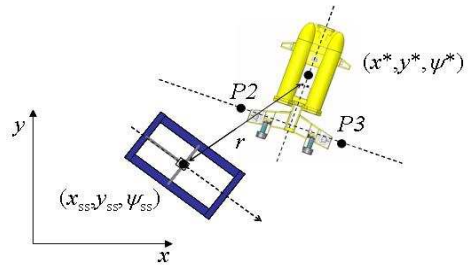
Stage 1 Docking

In this docking phase, the ASV and target are separated by a relatively large distance, typically beyond detection by the ASV vision system. In this case, GPS positions are typically used to define the target and ASV positions.

Through the wireless exchange of position and heading information between the ASV and target, this stage moves the ASV to a position directly behind the target to assist with the final alignment conducted in *Stage 2*. Figure 8(a) illustrates the *Stage 1* scenario where the actual target location and orientation is given by $(x_{sb}, y_{sb}, \psi_{sb})$, however, the desired position is set at a distance d_1 directly behind the target at point $P1$ where $\psi^* = \psi_{sb}$.



(a) Stage 1



(b) Stage 2

Figure 8: The two stages of ASV docking with a target using virtual force fields.

In this docking stage, there are two virtual forces acting. The first is a linear attraction force (F_{a1}) located at $P1$, with the other force, a repelling force (F_{r1}), located at the actual

target center-of-gravity. The repelling force is used avoid any collision between the ASV and the target. The Cartesian coordinates of $P1$ are given by:

$$x_1 = x^* + d_1 \sin(\psi^* + \pi) \quad (6)$$

$$y_1 = y^* + d_1 \cos(\psi^* + \pi) \quad (7)$$

Using Equation (7), both the attraction and repelling forces acting on the ASV are calculated. To ensure the virtual forces exerted on the vehicle do not exceed the ASV's capability, they are each clipped such that

$$F = \min(F, F_{max}) \quad (8)$$

where F_{max} is the maximum available thruster force, and F is the repelling and attracting forces considered individually.

These two virtual forces are then resolved into their respective Cartesian components by considering their line-of-action between their point source and the ASV, (F_{a1x}, F_{a1y}) and (F_{r1x}, F_{r1y}) respectively.

The resulting force vector acting on the ASV is the linear superposition of the individual virtual forces resolved in the global Cartesian coordinate system such that

$$\mathbf{F} = F_x \mathbf{i} + F_y \mathbf{j} \quad (9)$$

where $F_x = F_{a1x} + F_{r1x}$ and $F_y = F_{a1y} + F_{r1y}$.

When the ASV reaches a point that is within a pre-specified radius (d_{stage2}) of $P1$, the docking controller switches to *Stage 2*.

Stage 2 Docking

The second phase of docking allows the ASV to appropriately align with the target before moving over it to complete the manoeuvre. In this case, the vision system is typically used to achieve the finer control required to dock with the target.

Figure 8(b) illustrates the Stage 2 docking scenario. In this case, the desired position is set to the actual target position with a strong linear attracting virtual force set to this location. Additionally, there are two repelling virtual forces set perpendicular to the alignment axes at a distance d_s behind and perpendicular the target as denoted by points $P2$ and $P3$. These points are defined by:

$$d_s = \max(d_{min}, \alpha r) \quad (10)$$

$$x_{2,3} = x^* + d_s \sin(\psi^* \pm \pi/2) \quad (11)$$

$$y_{2,3} = y^* + d_s \cos(\psi^* \pm \pi/2) \quad (12)$$

where d_{min} and α are constants.

The resulting virtual force vector acting on the ASV is again a superposition of the three Stage 2 virtual forces resolved into the global Cartesian coordinate system.

4.2 Thruster Control

The vehicle's thruster controller was designed such that it would be biased towards yaw control to allow the ASV to appropriately turn towards the target and to try and reduce the total distance travelled. The demanded ASV heading angle (ψ_F) is set to align with the resulting virtual force vector acting on the vehicle such that

$$\psi_F = \tan^{-1} \left(\frac{F_x}{F_y} \right) \quad (13)$$

The demanded vehicle rotational force is then determined based on a proportional controller such that

$$F_\psi = \frac{2K_\psi(\psi_F - \psi)}{w} \quad (14)$$

where w is the distance between the thrusters, K_ψ is a constant of proportionality. This rotation (yawing) force is then clipped such that $(-F_{max} \leq F_\psi \leq F_{max})$.

The remaining available thrust is then converted to forward motion such that

$$F_v = F_{max} - |F_\psi| \quad (15)$$

The individual thruster forces are therefore determined by

$$F_L = (F_v + F_\psi) / 2 \quad (16)$$

$$F_R = (F_v - F_\psi) / 2 \quad (17)$$

$$(18)$$

5 Experimental Results

A series of experiments were conducted with the Starship ASV using the vision and docking strategies presented above. In these trials, the Starbug AUV [Dunbabin *et al.*, 2005] was used as a passive target, however, it could wirelessly communicate its GPS location and heading angle to the ASV for alignment.

5.1 Pool trials

The first set of trials consisted of controlled pool experiments to validate the vision-based target identification and vehicle control systems, as well as the docking strategy. Here the target (AUV) was placed at one end of the pool and the ASV placed randomly elsewhere in the pool. The ASV was then remotely instructed to dock with the target.

Figure 9(a) shows the ASV midway through a docking manoeuvre with the AUV where it has aligned with, and preparing to moving over the target. Figure 9(b) shows the relative segmented target image from the vision system for the instance shown in Figure 9(a).

The relative position of the target in the vehicle fixed coordinate frame is shown in Figure 10 for two representative docking experiments with different initial start conditions. Here it can be seen that with differing initial conditions, the



(a) ASV and AUV in pool (b) Segmented target image

Figure 9: Typical pool experiment showing the ASV during docking with the AUV. Also shown is the segmented image from the vision system.

control system manoeuvres the vehicle to get it close to the alignment axis ($y = 0$) before moving forward towards the target.

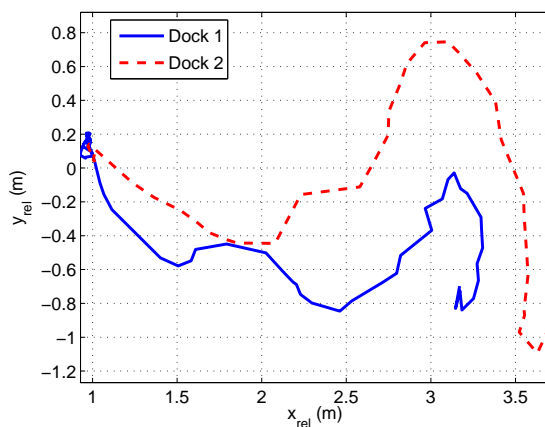


Figure 10: Measured target position with respect to the ASV coordinate frame during two docking experiments in the pool at different starting positions and orientations.

Figure 11 shows an image taken after the completion of a docking experiment with the AUV. Here it can be seen that the ASV has aligned with, and centered the target before moving over it to complete the docking procedure.

As the pool was relatively small, the close proximity of the target to the ASV meant that the system typically started in the second stage of docking. In order to test both stages of docking, a series of lake experiments were conducted.

5.2 Lake trials

A series of experiments were performed on Springfield Lake in Brisbane, Australia. Similar to the pool experiments, the target's GPS position and heading angle were wirelessly sent to the ASV and the vehicle then commanded to perform a docking manoeuvre. Figure 12(a) shows the GPS recorded track of the ASV during a representative docking. The location of the target (base) is indicated along with the *stage 2* switching boundary. The desired alignment angle was North.



Figure 11: The Starship ASV after docking with the AUV during a pool experiment.

Figure 12(b) shows the recorded ASV heading angle during docking manoeuvre where it can be seen that after 20s, the vehicle enters the second stage of the docking with the ASV's heading angle then approaching the desired alignment angle.

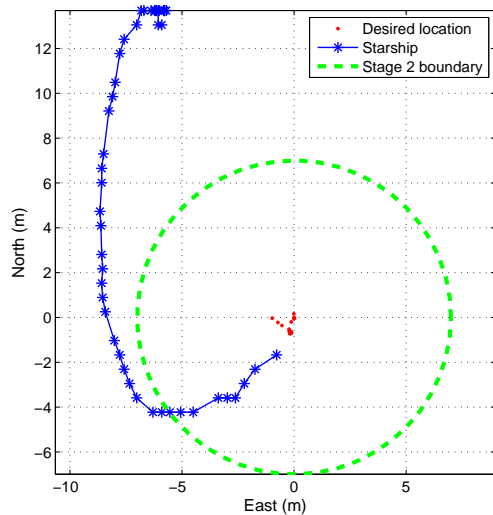
A number of problems were observed in these experiments primarily relating to the performance of the vision system. Due to the relatively high turbidity (muddiness) of the water, it was observed light reflecting from surface waves was sometimes falsely identified as a target. Solutions to improve performance of the vision system in this environment are a current area of research.

6 Conclusions

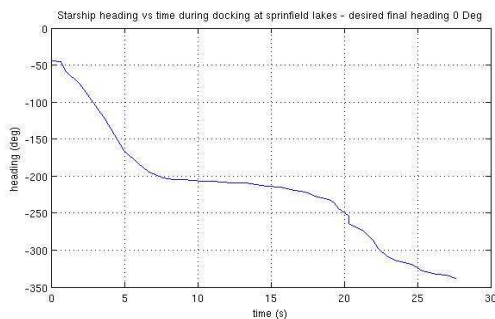
A novel approach to coordinated docking between an Autonomous Surface Vehicle (ASV) and an Autonomous Underwater Vehicle (AUV) has been presented. A real-time vision-based target identification system was developed and implemented on a low-power processor. The processed target coordinates are sent serially to the ASV controller, another low-power processor, which performs all vehicle control, sensor integration, and mission execution. The docking control strategy, based on virtual forces, allow obstacles to be introduced and avoided. The docking manoeuvres consisted of a two stage approach; the first moves the ASV to a pre-specified location using GPS or until the target is visually identified, with the second stage allowing alignment with, and then moving over, the target. The approach allows for passive (immobile) or active targets, that may or may not wirelessly communicate with the ASV. Experimental trials in a pool and lake have shown that the system is capable of autonomous docking with a surfaced AUV.

Acknowledgment

The authors would like to thank the contributions of other members of the CSIRO ICT Centre Autonomous Systems Laboratory: Cedric Pradalier, Les Overs, Polly Alexander



(a) ASV trajectory



(b) ASV heading angle

Figure 12: Measured GPS position and heading angle of the ASV during a representative lake experiment.

and John Whitham. Also, thanks goes to Alistair Grinham from the University of Queensland for his assistance during vehicle field trials.

References

- [Alves *et al.*, 2006] J. Alves, P. Oliveira, R. Oliveira, A. Pascoal, M. Rufino, L. Sebastiao, and C. Silvestre. Vehicle and mission control of the DELFIM autonomous surface craft. In *Proc. 14th Mediterranean Conference on Control and Automation*, pages 1–6, June 2006.
- [Bishop, 2004] B. Bishop. Design and control of platoons of cooperating autonomous surface vessels. In *Proc. 7th Annual Maritime Transportation System Research and Technology Coordination Conference*, November 2004.
- [Borenstein and Koren, 1989] J. Borenstein and Y. Koren. Real-time obstacle avoidance for fast mobile robots. *IEEE Transactions on Systems, Man, and Cybernetics*, 19:1179–1187, 1989.

- [Caccia, 2006] M. Caccia. Autonomous surface craft: prototypes and basic research issues. In *Proc. 14th Mediterranean Conference on Control and Automation*, pages 1–6, June 2006.
- [Corke *et al.*, 2004] Peter Corke, Pavan Sikka, Jonathan Roberts, and Elliot Duff. DDX: A distributed software architecture for robotic systems. In *Proc. Australian Conf. Robotics and Automation*, Canberra, December 2004.
- [Corke *et al.*, 2007] Peter Corke, Philip Valencia, Pavan Sikka, Tim Wark, and Leslie Overs. Long-duration solar-powered wireless sensor networks. In *Proc. Emmets, Cork*, June 2007.
- [Cucchiara *et al.*, 2003] R. Cucchiara, C. Grana, A. Prati, and R. Vezzani. A hough transform-based method for radial lens distortion correction. In *Proc. 12th International Conference on Image Analysis and Processing*, 2003.
- [Curcio *et al.*, 2005a] J. Curcio, J. Leonard, and A. Patrikalakis. SCOUT - a low cost autonomous surface platform for research in cooperative autonomy. In *Proc. MTS/IEEE OCEANS 2005*, pages 725–729, September 2005.
- [Curcio *et al.*, 2005b] J. Curcio, J. Leonard, J. Vaganay, and A. Patrikalakis. Experiments in moving baseline navigation using autonomous surface craft. In *Proc. MTS/IEEE OCEANS 2005*, pages 730–735, September 2005.
- [Dunbabin *et al.*, 2005] Matthew Dunbabin, Jonathan Roberts, Kane Usher, Graeme Winstanley, and Peter Corke. A hybrid AUV design for shallow water reef navigation. In *Proceedings of the 2005 International Conference on Robotics and Automation*, pages 2117–2122, Barcelona, April 2005.
- [Larson *et al.*, 2006] J. Larson, M. Bruch, and J. Ebken. Autonomous navigation and obstacle avoidance for unmanned surface vehicles. In *Proc. SPIE Unmanned Systems Technology VIII*, April 2006.
- [Leonessa *et al.*, 2003] A. Leonessa, J. Mandello, Y. Morel, and M. Vidal. Design of a small, multi-purpose, autonomous surface vessel. In *Proc. OCEANS 2003*, pages 544–550, 2003.
- [Manley *et al.*, 2000] J.E. Manley, A. Marsh, W. Cornforth, and C. Wiseman. Evolution of the autonomous surface craft AutoCat. In *Proc. MTS/IEEE OCEANS 2000*, pages 403–408, September 2000.
- [Martins *et al.*, 2007] A. Martins, J.M. Almeida, H. Ferreira, H. Silva, N. Dias, A. Dias, C. Almeida, and E.P. Silva. Autonomous surface vehicle docking manoeuvre with visual information. In *Proc. International Conference on Robotics and Automation*, pages 4994–4999, April 2007.
- [Pascoal *et al.*, 2000] A. Pascoal, P. Oliveira, C. Silvestre, L. Sebastiao, M. Rufino, V. Barosso, J. Gomes,

- G. Ayela, P. Coince, M. Cardew, A. Ryan, H. Braithwaite, N. Cardew, J. Trepel, N. Seube, J. Champeau, P. Dhaussy, V. Sauce, R. Moitie, R. Santos, F. Cardigos, M. Brussieux, and D. Dando. Robotic ocean vehicles for marine science applications: the european asimov project. In *Proc. MTS/IEEE OCEANS 2000*, pages 409–415, September 2000.
- [Reed *et al.*, 2006] C.M. Reed, B.E. Bishop, and J.K. Waters. Hardware selection and modelling for a small autonomous surface vessel. In *Proc. 38th Southeastern Symposium on System Theory*, pages 196–200, March 2006.
- [Reyhanoglu and Bommer, 2006] M. Reyhanoglu and A. Bommer. Tracking control of an underactuated autonomous surface vessel using switched feedback. In *Proc. IECON 2006*, pages 3833–3838, November 2006.
- [Smith, 1978] A.R. Smith. Color gamut transform pairs. In *IGGRAPH '78: Proceedings of the 5th annual conference on Computer graphics and interactive techniques*, pages 12–19, 1978.
- [Vaneck, 1997] T.W. Vaneck. Fuzzy guidance controller for an autonomous boat. *Control Systems Magazine*, 17:43–51, 1997.